Eidgenössische Technische Hochschule Zürich
Swiss Federal Institute of Technology Zurich

Design and Construction of Spectral Filters for Quantum Transduction with Fast Feedback

Project Report

Vinícius Mohr
vimohr@ethz.ch

Laboratory for Solid State Physics
Departement of Physics, D-PHYS
ETH Zürich

Supervisors:
Prof. Dr. Yiwen Chu
Maxwell Drimmer

October 5, 2023

Abstract

In the pursuit of efficient microwave-to-optical transduction, optomechanical transducers have emerged as a promising avenue due to the high spatial overlap between microwave phonons in certain materials and optical photons, facilitated by their similar wavelengths. However, the presence of pumping light required poses a challenge that hinders the accurate processing of the transduced quantum state. To address this issue, we have taken initial steps toward building an optical filter cavity system with fast locking capabilities. Our system achieved transmissions of over 85% and 90% for the two Fabry-Pérot cavities. In addition, we performed a thorough characterization of the primary loss sources in the setup and made linewidth and free spectral range measurements of one cavity. These results provide a basis for further improvements of the filter system and pave the way for more efficient microwave-to-optical tranduction in the future.

Contents

Chapter 1

Introduction

Improving communication between quantum computers is a critical step in advancing quantum computing and making it more practical. Optical photons, similar to their use in current telecommunication networks, appear to be the most suitable medium for this purpose. Optical photons have long coherence times, even at room temperature, allowing them to carry quantum information for long periods of time. Moreover, these photons can be transmitted through optical fibers with minimal loss, making long-distance quantum information transport a feasible possibility.

However, a challenge arises when attempting to directly transfer quantum information from qubits that operate on microwave frequency photons (such as superconducting circuits or color centers) to optical photons. The significant difference in energy scales between optical photons and the qubits leads to either disruption of the systems or absence of any interaction when attempting to couple them. To circumvent this limitation, an intermediary system becomes essential [1]. Among the available alternatives, the optomechanical approach, which leverages mechanical degrees of freedom, presents itself as a promising contender [2].

A major milestone in the development of this approach is the $\hbar$BAR. This innovative device enables the quantum state conversion from a microwave frequency controlled qubit (such as a superconducting circuit [3]) to a mechanical resonator. This conversion is achieved by a SWAP-like electromechanical coupling between a piezoelectric transducer and the electric microwave field.

Using a three-wave mixing mechanism inside a Fabry-Pérot cavity (see Figure 1.1), we can then effectively convert the mechanical mode excitations generated by the $\hbar$BAR into optical mode excitations via Brillouin scattering. In this process, a pump photon (red) and a phonon (green) are annihilated, while a probe photon (blue) is coherently excited, preserving quantum information throughout the process.

By using a strong coherent laser drive as the source for the pumping light, this process can be described with a SWAP-like Hamiltonian, as elaborated in [4]:

$$\hat{H}_{\text{eff}} = \hbar\Omega g_{\text{eff}}\hat{a}\hat{b}^{\dagger} + \hbar\Omega^{*} g_{\text{eff}}^{*}\hat{a}^{\dagger}\hat{b}, \tag{1.1}$$

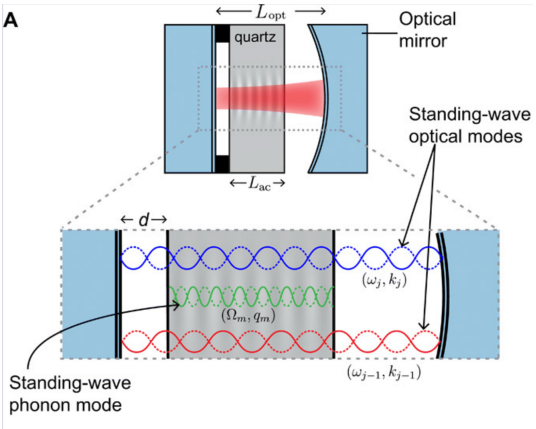

Figure 1.1.: Fabry–Pérot cavity with optomechanical coupling (from [7])

where $\hat{a}$ and $\hat{a}^\dagger$ are the annihilation and creation operators for the excited photon mode, and $\hat{b}$ and $\hat{b}^\dagger$ are the phonon annihilation and creation operators. The parameters Ω and g_{eff} represent the coherent pumping laser drive and the coupling strength, respectively.

Despite their large difference in frequency, microwave phonons (with a sound velocity of $\sim 10^4$m/s) and optical photons (moving at the speed of light at about $\sim 10^8$m/s), can still be involved in a three-wave mixing process that conserves momentum. Due to the significant spatial overlap between the mechanical and optical modes inside the cavity, the optomechanical coupling mechanism allows to achieve a substantial interaction strength, characterized by a cooperativity value larger than 1 [5].

However, there is a problem to deal with. The light exiting the cavity is a mixture of both photon frequencies. Since the quantum information is only stored in the probe photons excited inside the cavity, and the relative frequency difference between the two photon modes is small, it is essential to filter out the pump (red) light while minimizing losses of the other frequency. Our estimates show that the intensity of the desired light is smaller by an order of 10^8 compared to the pump light, which means that the pump light has to be suppressed by more than 80 dB. Here we actually aim for a suppression of about 120 dB, since this should result in a sufficiently low error rate while still being feasible.

To achieve effective filtering, we plan to implement a system of three successive cavities with each having the ability to lock to a frequency, closely following the setup used by the Gröblacher group [6]. This configuration aims to efficiently filter out the pumping light and retain the desired frequency for quantum information transmission.

Chapter 2

Setup

In our setup, shown in Figure 2.1, we use a near-infrared (NIR) laser with a wavelength of about 1550 nm that is capable of sweeping over multiple frequencies and locking to a specific frequency using a Pound-Drever-Hall (PDH) lock. These features are extremely valuable for the alignment process.

The selected frequency of the laser closely matches the frequency of the photons generated during the optomechanical transduction, making the alignment behavior a predictor of future performance with the correct light mixture. Achieving precise alignment of the spatial characteristics of the incident light with the radius of curvature and length of the cavity is essential for optimal light coupling. This is achieved by carefully selecting both the beamwidth of the laser and the focal length of the focusing lens.

First, the light emitted from the laser source and transmitted through the fiber undergoes polarization adjustment to achieve nearly linear polarization before exiting the fiber. However, we found that the beamwidth of the light after collimation (2.84 ± 0.02 mm) was much smaller than the 3.2 mm required for the cavity. To address this, we designed a Keplerian telescope incorporating two plano-convex lenses, effectively increasing the beamwidth to 3.27 ± 0.02 mm, which is much closer to the desired value.

Next, we added a linear polarizing beamsplitter and a quarter-wave plate to the setup. Together with the cavity, which reflects some of the light, and a photodetector connected via a fiber, this configuration functions as a circulator. Light passing straight through the beamsplitter has a specific linear polarization. By setting the fast axis of the quarter-wave plate at an angle of $\pi/4$ to it, the light becomes circularly polarized after passing through it once. Upon reflection from the cavity and a second passage through the quarter-wave plate, the polarization becomes orthogonal to the transmitted polarization. As a result, it is reflected at the beamsplitter, directed to a mirror, coupled into a fiber, and finally reaches a photodiode. Initially, this signal stabilizes the light to a main cavity mode using the PDH lock, improving transmission through the cavity and facilitating alignment of the second cavity. However, the long-term goal is to use this signal to lock the cavity length by manipulating one of its mirrors using a piezoelectric element [8]. This capability is critical because the light frequency entering the cavity system depends on both the pumping light frequency and the phonon frequency of the preceding optomechanical cavity.

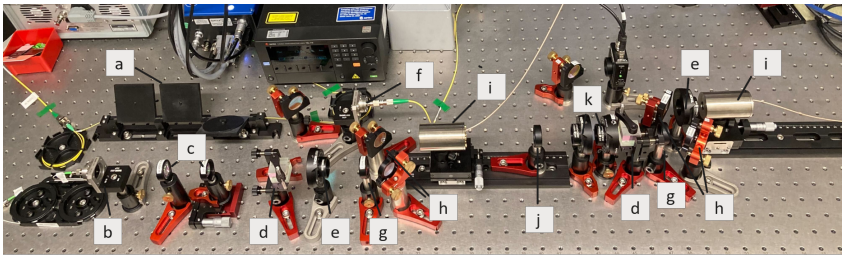

Figure 2.1.: The setup we built so far (up to the second cavity). a: Polarization Controller, b: fiberport collimator, c: Keplerian telescope, d: polarizing beamsplitter, e: quarter-wave plate, f: fiberport coupler, g: plano-convex lens, h: IR dielectric concave mirrors, i: Fabry-Pérot cavity with piezo actuator, j: plano-convex lens, k: quarter- and half-wave plate

Following the quarter-wave plate, a plano-convex lens precisely focuses the light into the first filter cavity. Two mirrors are positioned to optimize the light path, increasing the intensity of the outgoing light for the fundamental mode frequencies. The procedure for achieving this optimized path is discussed in detail in the upcoming chapter. Another plano-convex lens collimates the outgoing beam. Additional quarter-wave and half-wave plates are inserted immediately after this lens to compensate for the expected circular polarization of the light exiting the cavity. Converting it to linear polarization minimizes losses when the light passes through the subsequent beamsplitter. The remaining components of the setup mirror those employed in the initial section.

Chapter 3

Cavity alignment techniques

In this chapter, we aim to provide a comprehensive overview of the methods used to align the two cavities and achieve high transmission. The alignment process can be divided into two main steps.

The first step is to position the Fabry-Pérot cavity, which consists of two plano-concave mirrors with the same radius of curvature (30 mm), so that its center is precisely located at the focal point of the incident light. This ensures optimal coupling between the light and the cavity.

The second step involves carefully adjusting the mirror angles to obtain the ideal path for the light to travel through the cavity. By fine-tuning the mirror angles, we can optimize the trajectory of the light to maximize its transmission through the cavity.

3.1. Cavity positioning

In order to achieve precise placement of the cavity, we have set up a rail system on which the cavity will be positioned. Before placing the cavity, we take several beamwidth measurements using the razor blade method [9, pp. 33–36]. These measurements capture the beam diameters at different positions along the rail. We then fit these beamwidth measurements to the standard beam evolution of a Gaussian beam using the following formula for the beam diameter as a function of the location z [10, pp. 81–83]:

$$w(z) = w_0 \sqrt{1 + \left(\frac{z - z_0}{z_R} \right)^2}, \tag{3.1}$$

where w_0 is the waist diameter, z_R corresponds to the Rayleigh range, and z_0 is the location of the beam waist that we wish to determine. A plot illustrating this relationship can be seen in 3.1. The calculated value of z_0 is then used as the designated location for the center of the cavity.

3.2. Mirror alignment

Once the cavity is properly positioned, optimizing the laser path through the cavity becomes critical to maximize the transmission of the fundamental Gaussian mode [11,

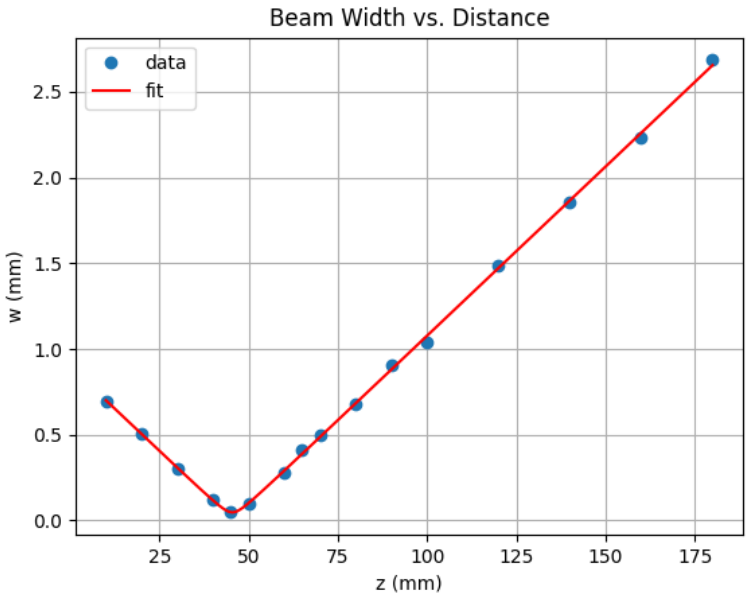

Figure 3.1.: The beam diameters measured at multiple locations on the rail and fitted to a Gaussian beam evolution

pp. 330–339]. The first step is to connect the piezoelectric element of the cavity to a waveform generator, with an amplifier in between, enabling periodic sweeping of the cavity length while maintaining a constant laser frequency. To assess the laser path, we observe the reflected light beam using a fluorescence card (THORLABS VRC4), as shown in Figure 3.2a. The mirrors are then adjusted to closely align the incoming and reflected light.

Continuing the alignment process, the focus shifts to the outgoing beam. However, the transmitted intensity is currently low, making it difficult to see any light coming out of the cavity. To solve this problem, we employ an EDFA (Erbium-doped Fiber Amplifier) to increase the total laser intensity to 170 mW, and we use a different fluorescence card (THORLABS VRC2) that has a higher sensitivity to low light levels and saturates faster.

These adjustments then allow us to visualize the ellipsoidal shape of the transmitted beam, as shown in Figure 3.2b. This shape corresponds to a superposition of Gaussian modes that are excited in the cavity. Since the goal is to maximize the transmission through the cavity, we need to enhance the contribution of the fundamental mode, which corresponds to a point-like beam shape.

To achieve this, the first step is to gradually reduce the size of the ellipsoid by making small adjustments to one of the mirrors. Next, the "beam-walking" technique is

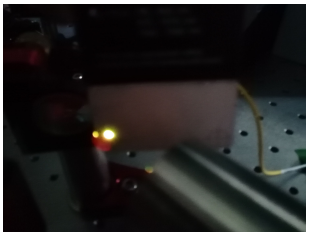

a Reflected laser beam (right and bright) does not line up with the incoming laser beam (left and weaker)

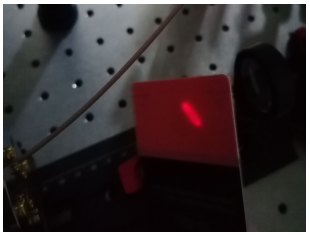

b Ellipse shaped "beam" coming out of the cavity

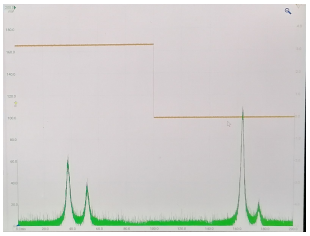

c Transmission spectrum coming out of the first cavity before optimizing the beam path (measured using a powermeter)

Figure 3.2.

used, in which one mirror is rotated in a certain direction to increase the size of the ellipsoid, followed by compensating for the effect by adjusting the other mirror accordingly (vertical adjustments require turning both gears in the same direction, while horizontal adjustments require opposite rotations). This iterative process causes the minimum size of the ellipsoid to vary, either decreasing or increasing. If the size increases, the beam must be "walked" in the opposite direction. At some point, the ellipse may become so small that it is barely visible by eye.

To overcome this, a photodetector (such as a powermeter) connected to an oscilloscope is used to analyze the light transmitted through the cavity. The oscilloscope should show transmission peaks, like in Figure 3.2c. The beam-walking procedure is then repeated, but instead of minimizing the size of the ellipse, efforts are focused on maximizing the size of the highest peaks corresponding to the fundamental mode.

The results obtained with this approach are shown in Figure 3.3. However, achieving transmissions of about 85% or 90% falls short of our requirements, since more than 10% of the light is lost at each cavity. Based on the research of the Gröblacher group [6], we expect that transmissions in the range of 98-99% are achievable.

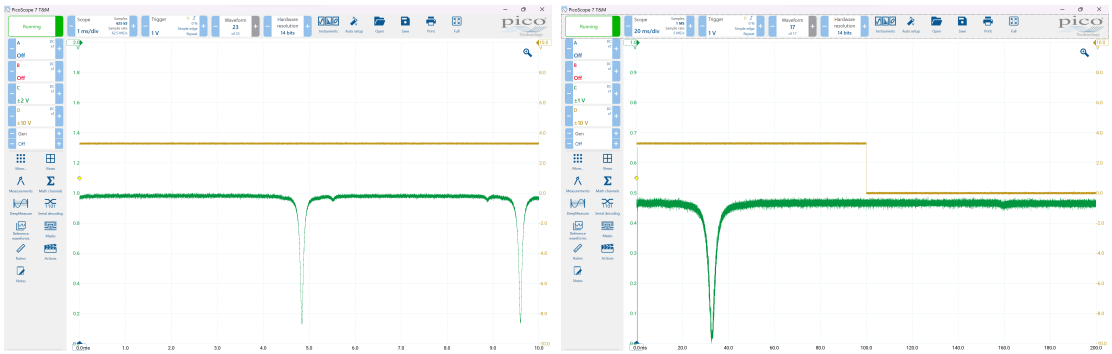

Figure 3.3.: The measured intensity is shown in green on the left (right) while sweeping at location 3 (7) (see figure 4.2) after aligning cavity 1 (2) with an approximate transmission of 85% (90%). The yellow line represents the trigger signal of the sweeping.

Chapter 4

Further Measurements

4.1. Error characterization

To evaluate the overall transmission, we used a power meter to measure the light intensity at different positions, as shown in Figure 4.2. Positions 1-4 were measured while varying the laser frequency and keeping the length of the first cavity constant. Conversely, positions 5-8 were measured while using light locked to the first cavity via the Pound-Drever-Hall (PDH) lock and sweeping the length of the second cavity using the piezo actuator. The results of these measurements are shown in Figure 4.1.

First, it is important to note that the measurements at positions 3 and 7 are primarily relevant to future cavity locking. As long as the intensity does not drop of by a large amount, the losses can be ignored. The transitions from positions 2 to 4 and from 6 to 8 show small losses of a few hundredths of a dBm, which are not critical. Conversely, the transitions from positions 1 to 2 and from 5 to 6 exhibit losses of about 0.47 dBm and 0.25 dBm, respectively. These losses have a significant impact on the total loss and should be addressed, for example, by improved light polarization control to mitigate the significant light loss caused by reflection at the beamsplitter.

The most substantial loss occurs between positions 4 and 5 within the first cavity, resulting in a loss of approximately 1.43 dBm, despite being stabilized by the PDH lock. This corresponds to a transmission of roughly 70%, which is significantly lower than the previously measured 85% during the sweeping process (see Figure 3.3). A possible reason for this discrepancy could be an imperfect alignment of the PDH lock to the maximum.

In total, approximately 2.22 dBm of the initial intensity is lost before entering the second cavity. By improving light polarization control, cavity alignment, and the locking system, these losses can be significantly reduced.

No	Intensity in mW	Intensity in dBm
1	173.8 ± 0.5	22.40 ± 0.02
2	156.0 ± 0.5	21.93 ± 0.02
3	137.9 ± 0.5	21.40 ± 0.02
4	154.3 ± 0.5	21.88 ± 0.02
5	111.0 ± 0.5	20.45 ± 0.02
6	104.6 ± 0.5	20.20 ± 0.02
7	98.4 ± 0.5	19.93 ± 0.02
8	104.3 ± 0.5	20.18 ± 0.02

Figure 4.1.: Light intensity measurements at different locations in mW and dBm

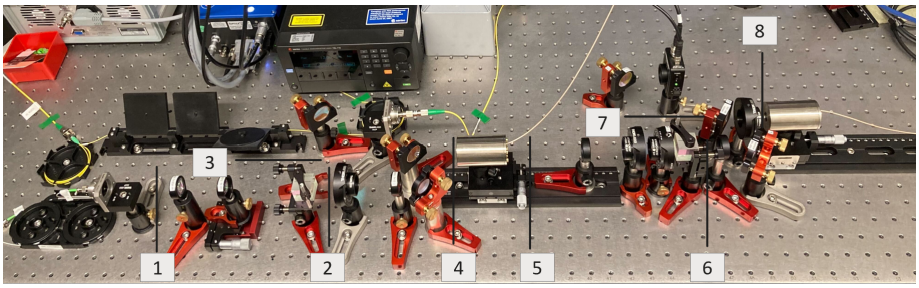

Figure 4.2.: Our setup with highlighted intensity measurement locations

4.2. Linewidth and FSR measurements

To measure the free spectral range (FSR) or the linewidth (FWHM) with an oscilloscope, a method is needed to convert the displayed time differences into effective frequency differences. This allows direct estimation of these two values.

To accomplish this, we use a reference cavity with a known FSR of 93.2 MHz. The incoming laser light is split, with one portion passing through the reference cavity and the other through the cavity under investigation. The outgoing intensities from both cavities are measured using a photodiode connected to an oscilloscope (see Figure 4.4). Since the FSR of the reference cavity is known, the time interval can be expressed as a frequency difference.

However, it is important to consider variations in the peak-to-peak distances over time, as shown in the reflection spectrum of the reference cavity (see Figure 4.5). Since the FSR of the reference cavity is significantly smaller than that of the filter cavity, we can conveniently determine the frequency estimate by counting the number of reference cavity peaks within the time domain in which we want to estimate the frequency. Using this method, we obtain an FSR of 19.3 ± 0.3 GHz, which is significantly lower than our intended target of 26.2 GHz. This indicates that the cavity length is too long, which could be corrected by removing a few spacers from inside the cavity.

In addition, the same approach can be used to approximate the linewidth. For each dip, we measure the width at the midpoint between the baseline and the dip height (as shown in Figure 4.6). The linewidth is then described as a non-integer multiple of the reference FSR, corresponding to the peak-to-peak distances on the blue line. As a result, we obtained the following linewidth values for each of the four dips (Figure 4.3).

Peak	Linewidth (MHz)
1	87.4 ± 4.4
2	92.4 ± 4.7
3	89.2 ± 4.5
4	84.6 ± 4.3

Figure 4.3.: Linewidths for each of the dips in the reflection spectrum. An error of 5% is assumed to account for the imprecise measuring (about one reference FSR fits inside a dip) and slight deviation from a Lorentzian shape.

Unfortunately, the obtained linewidths of about 90 MHz are significantly lower than the expected value of 160 MHz calculated with a reflectivity of 98% given by the manufacturer. The error of the reflectivity value, which is $\pm 0.1\%$, does not even come close to explaining the significant deviation of about 45%. This situation strongly suggests the presence of a significant flaw in our analytical approach that needs to be further investigated.

In addition to this discrepancy, the estimated linewidths differ by as much as 10%, although they are expected to be more or less identical. However, a simple way to improve the variation of our linewidth estimates is to perform multiple measurements and then calculate the average, which would reduce the errors due to sweeping rate fluctuations.

In addition, one could fit the reflectivity dips with a Lorentzian function. However, it is worth noting that the time-frequency relationship, as shown in Figure 4.5, exhibits substantial local variability, making it problematic to approximate with a simple linear model. To address this problem effectively, one can use more sophisticated models, such as higher order polynomials or Fourier analysis, which would provide a better approximation of the frequency-time dependence and thus improve the estimate.

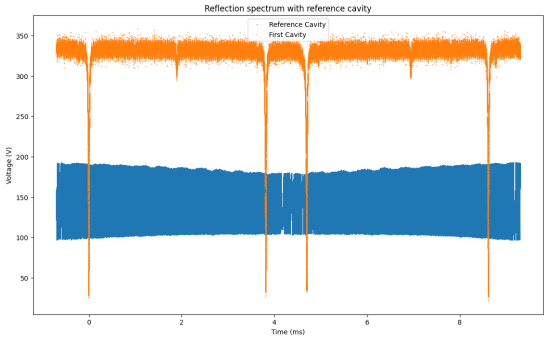

Figure 4.4.: Reflection spectrum of the reference cavity (blue) and the first cavity (orange), measured using a photo diode and an oscilloscope. As the laser is sweeping its frequency up and down, the right half should be a mirror image of the left.

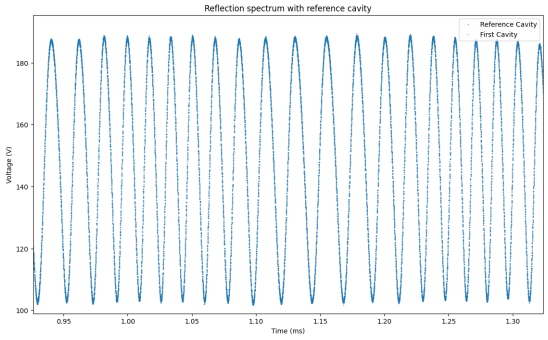

Figure 4.5.: Reflection spectrum of the reference cavity for a shorter time frame

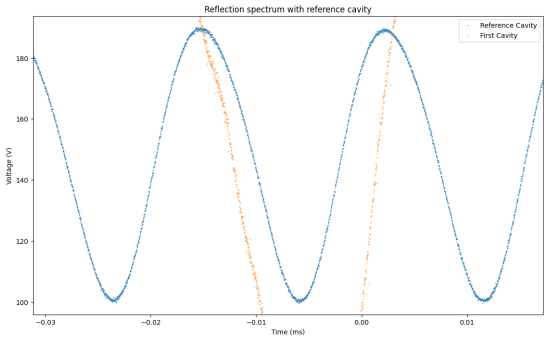

Figure 4.6.: Figure 4.4 zoomed at the first dip of the first cavity

Chapter 5

Conclusion

The primary goal of this project was to take the first steps toward creating a precise frequency filtering system capable of locking on to a specific frequency. The locked system should allow light of the desired frequency to pass while significantly reducing the intensity of the unwanted pumping light, which has an about eight orders of magnitude higher intensity and a frequency difference of only a few GHz compared to the light we want to measure. This filtering process is critical for efficient microwave phonon to optical light conversion as it allows us to effectively remove the pumping light and perform a single-photon measurement on the newly created light.

Closely following the Gröblacher setup (Figure **??**), we have successfully replicated an analogous setup up to the second cavity. Using the razor blade method, we were able to accurately estimate the beam diameter evolution along the optical axis, allowing for precise placement of the cavities. By carefully adjusting the laser path, we achieved transmission rates of about 85% for the first cavity and 90% for the second cavity (Figure 3.3). Our analysis showed that the main sources of light loss were the beamsplitters (about 0.3 dBm) and, in particular, the suboptimal cavity transmission (approximately 1.2 dBm for the first cavity).

Going forward, several critical steps should be considered for the continuation of the project. First, the development of fast and precise cavity locking is essential to efficiently align the third cavity and improve transmission when locked. As observed, the transmission through the first cavity decreased by approximately 15% when locked compared to the maximum transmission during sweeping, underscoring the importance of implementing an effective cavity locking mechanism. Second, additional linewidth measurements will provide valuable insight into the adequacy of light filtering at the pumping frequency. A proper linewidth is critical, as an excessive linewidth can result in undesirably high transmission of unwanted frequencies. Finally, improving polarization control in the setup would significantly reduce losses at the beamsplitter by optimizing the polarization of the light.

This project and future efforts in this direction may lead to an efficient method for microwave to optical transduction, further underscoring the importance of mechanical systems in quantum information processing and the development of a quantum network.

Appendix A

Used Codes

To obtain the data points for the razor blade measurement I used the grinlens-measurement script which can be found on the group drive:

```
Z:\\3 - codes\\_GitLab_Controlled\\grinlens-measurement-software
```

The other codes, for fitting the error function (fit_error_function.py) to get the beam diameter, for fitting the beam diameters to the beam evolution of a Gaussian beam (fit_gaussian_beam.py), and for fitting a Lorentzian to the reflection or transmission peaks (fit_lorentzian.py), can be found on the group drive as well:

```
Z:\\3 - codes\\23-07-16_Vini_Code
```

Bibliography

1. Lauk, N. *et al.* Perspectives on quantum transduction. *Quantum Science and Technology* **5,** 020501. https://dx.doi.org/10.1088/2058-9565/ab788a (Mar. 2020).
2. Chu, Y. & Gröblacher, S. A perspective on hybrid quantum opto- and electromechanical systems. *Applied Physics Letters* **117,** 150503. https://doi.org/10.1063%2F5.0021088 (Oct. 2020).
3. Chu, Y. *et al.* Quantum acoustics with superconducting qubits. *Science* **358,** 199–202. https://www.science.org/doi/abs/10.1126/science.aao1511 (2017).
4. Aspelmeyer, M., Kippenberg, T. J. & Marquardt, F. Cavity optomechanics. *Rev. Mod. Phys.* **86,** 1391–1452. https://link.aps.org/doi/10.1103/RevModPhys.86.1391 (4 Dec. 2014).
5. Doeleman, H. M. *et al. Brillouin optomechanics in the quantum ground state* 2023. arXiv: 2303.04677 [quant-ph].
6. Zivari, A. *et al.* On-chip distribution of quantum information using traveling phonons. *Science Advances* **8,** eadd2811. https://www.science.org/doi/abs/10.1126/sciadv.add2811 (2022).
7. Kharel, P. *et al.* High-frequency cavity optomechanics using bulk acoustic phonons. *Science Advances* **5,** eaav0582. https://www.science.org/doi/abs/10.1126/sciadv.aav0582 (2019).
8. *Low voltage HPSt150 piezo-ring actuators with preloaded casings* (). https://www.piezomechanik.com/fileadmin/content_files/products/actuators/actuators-3-piezo-ring-actuators-hpst150-tubular.pdf.
9. Vollenweider, S. *A cryogenic optical cavity for Brillouin cavity optomechanics* 2020. https://ethz.ch/content/dam/ethz/special-interest/phys/solid-state-physics/hyqu-dam/documents/master-thesis-silvan-vollenweider.pdf.
10. Bahaa E. A. Saleh, M. C. T. in *Fundamentals of Photonics* 80–107 (John Wiley & Sons, Ltd, 1991). ISBN: 9780471213741. https://onlinelibrary.wiley.com/doi/abs/10.1002/0471213748.ch3.
11. Bahaa E. A. Saleh, M. C. T. in *Fundamentals of Photonics* 310–341 (John Wiley & Sons, Ltd, 1991). ISBN: 9780471213741. https://onlinelibrary.wiley.com/doi/abs/10.1002/0471213748.ch9.

Eidgenössische Technische Hochschule Zürich
Swiss Federal Institute of Technology Zurich

Declaration of originality

The signed declaration of originality is a component of every semester paper, Bachelor's thesis, Master's thesis and any other degree paper undertaken during the course of studies, including the respective electronic versions.

Lecturers may also require a declaration of originality for other written papers compiled for their courses.

I hereby confirm that I am the sole author of the written work here enclosed and that I have compiled it in my own words. Parts excepted are corrections of form and content by the supervisor.

Title of work (in block letters):

Design and Construction of Spectral Filters for Quantum Transduction with Fast Feedback

Authored by (in block letters):

For papers written by groups the names of all authors are required.

Name(s):	**First name(s):**
Mohr	Vinicius

With my signature I confirm that

- I have committed none of the forms of plagiarism described in the 'Citation etiquette' information sheet.
- I have documented all methods, data and processes truthfully.
- I have not manipulated any data.
- I have mentioned all persons who were significant facilitators of the work.

I am aware that the work may be screened electronically for plagiarism.

Place, date	**Signature(s)**
Zurich, September 26th, 2023	

For papers written by groups the names of all authors are required. Their signatures collectively guarantee the entire content of the written paper.